BES Analysis Memo
Search for $\psi(2S)$ Decays to Vector plus Tensor Mesons

Li Xinhua
email: LIXH@bepc5.ihep.ac.cn
(Revised June 5, 1997)

Abstract

The hadronic decays $\psi(2S) \to \omega f_2$, ρa_2 $K^{*0}K_2^{*0}$ and $\phi f_2'(1525)$ have been studied in a sample of 3.7×10^6 $\psi(2S)$ events. Measurements of their branching fractions are presented. All channels violate the "15% *rule*" predicted by perturbative QCD compared with the corresponding J/ψ decays. As vector-tensor pair combinations, they provide the first anomalous example of non-vector-pseudoscalar decays of charmonium.

I. INTRODUCTION

There exists a long standing puzzle in the study of charmonium decays. According to Applequist and Politzer [1], there is a direct parallel between the decay of $\psi(2S)$ and J/ψ to three massless gluons

$$Q_h \equiv \frac{B(\psi(2S) \to ggg)}{B(J/\psi \to ggg)} = \frac{B(\psi(2S) \to e^+e^-)}{B(J/\psi \to e^+e^-)} = (14.6 \pm 2.2)\%$$

where the leptonic branching fractions from PDG [2] are used.

The Mark II first revealed unexpected small values for the ratios of $\psi(2S)$ to J/ψ branching fractions for decays to $\rho\pi$ and $K^{*\pm}K^{\mp}$. With a data sample of 1.02×10^6 produced $\psi(2S)$ events, it was found that $Q_{\rho\pi} < 0.63\%$ (90% *C.L.*) and $Q_{K^{*\pm}K^{\mp}} < 2.07\%$ (90% C.L.) [3].

Following Mark II, several radiative decays were measured by the Crystal Ball experiment [4]. Radiative decays of $\psi(2S)$ to the tensor f_2 was observed but neither to the η nor the η'. These results, in combination with the Mark II results, immediately led to a conclusion that the suppressed modes are just vector-pseudoscalar decays of $\psi(2S)$. Ever since it becomes popular in the literature to refer to the puzzle as "*vector − pseudoscalar puzzle*".

A number of theoretical models [5] have been suggested to explain the puzzle, but none of them are satisfactory.

This paper extends to the observation of vector-tensor combination decays, $\psi(2S) \to \omega f_2$, ρa_2 and $\phi f_2'$. Data were taken during 1993-1995 at the BEPC. The total event number of $\psi(2S)$ is $(3.7 \pm 0.3) \times 10^6$ got by observing the inclusive production of J/ψ in the process $\psi(2S) \to \pi^+\pi^- J/\psi$ and using the branching fraction of $\psi(2S) \to \pi^+\pi^- J/\psi$ of PDG [2].

II. $\psi(2S) \to \pi^+\pi^-\pi^+\pi^-\pi^0$ SELECTION

Events with four charged tracks (MFIT=2) in the polar angle region $-0.8 < \cos\theta < 0.8$ and with zero net charge have been selected. The dE/dx measurements are used to select pion tracks with confidence level larger than 0.003 for each track and 0.01 for all tracks combined. So are the TOF measurements of high quality ($T_{qual} = 1$). Moreover, at least two neutral tracks with polar angle $-0.75 < \cos\theta < 0.75$ are required for photon candidates.

Magnetic field correction is made to the momentum of charged track. Momentum corrections are further made for energy loss and multiple Coulomb scattering in the material before charged particles enter the drift volume in BES inner detector. So are photon directions entering shower counter for beam position dispersion in the colliding zone.

Events are kinematically $4C2\gamma$ fitted with all photon pairs. The pair with highest probability of fit are selected and it is also required to be greater than 0.01. The π^0 is selected by requiring the invariant mass of two photons to be $85 < M_{\gamma\gamma} < 205\ MeV/c^2$. Its side band is defined as the mass range $40 < M_{\gamma\gamma} < 80\ MeV/c^2$ and $210 < M_{\gamma\gamma} < 290\ MeV/c^2$. Several steps are processed to remove fake photon contamination. The angle between photon and charged track is larger than 13^o. The distance of photon and charged track hitting shower counter is larger than 35cm. The fitted energy of photon is higher than 60MeV.

Furthermore, the J/ψ contamination are removed by two steps. $M(\pi^+\pi^-) < 2.9\ GeV/c^2$ is to remove e^+e^- or $\mu^+\mu^-$ contamination from $\psi' \to \eta J/\psi$ where η decays to $\pi^+\pi^-\pi^0$ and J/ψ decays to leptons. No $\pi^+\pi^-$ combination is allowed to recoil to J/ψ within $50MeV/c^2$ of J/ψ mass to exclude the background $\psi(2S) \to \pi^+\pi^- J/\psi$ with J/ψ decaying to $\pi^+\pi^-\pi^0$.

III. ANALYSIS OF $\psi(2S) \to \omega\pi^+\pi^-$

The $\pi^+\pi^-\pi^0$ mass spectrum figure 1 shows significant ω signal. The similar plot of π^0 side band figure 2 shows invisible ω signal. The mass distribution is fitted to a Breit-Wigner curve with width fixed to PDG [2] and float mass added to a quaduatical background. Mass resolution is 13.4 MeV got by Monte Carlo simulation. The fit gives 118.0 ± 22.8 events and mass of ω $(781 \pm 2) MeV/c^2$ well consistent with PDG [2]. The efficiency is 0.076 calculated by Monte Carlo simulation with uniform phase space distribution. The branching fraction is obtained

$$B(\psi(2S) \to \omega\pi^+\pi^-) = (4.7 \pm 0.7 \pm 1.0) \times 10^{-4},$$

where the first error is statistical and second systematic. The systematic error mainly dues to the cut on kinematic fit. It also contains signal fit to different background line, the simulation of analysis efficiency, total number of $\psi(2S)$, and the branching fraction of $\omega \to \pi^+\pi^-\pi^0$ given by PDG [2]. So are calculated for the other systematic errors in this memo.

The $\omega\pi^+\pi^-$ candidates are selected by requiring $740 < m_{\pi^+\pi^-\pi^0} < 820\ MeV/c^2$. $680 < m_{\pi^+\pi^-\pi^0} < 720 MeV/c^2$ and $840 < m_{\pi^+\pi^-\pi^0} < 880 MeV/c^2$ are chosen for the ω side band. The Dalitz plot of $\omega\pi^+$ versus $\omega\pi^-$ are in figure 3 for ω mass region and figure 4 for the side band.

The $\omega\pi^\pm$ mass spectrum figure 5 shows a clear $b_1^\pm$ signal owing to the proximity of the phase space limit. The similar plot for the ω side band figure 6 shows very few $b_1^\pm$ signal.

The mass distribution is fitted to a Breit-Wigner curve with width fixed to PDG [2] and float mass added to a quaduatical background. Mass resolution is 12.3 MeV got by Monte Carlo simulation. The fit gives 68.7 ± 11.0 events and mass of $b_1^{\pm}$ $(1255 \pm 15) MeV/c^2$ consistent with PDG [2]. The efficiency is 0.07 calculated by Monte Carlo simulation with uniform phase space distribution. The branching fraction is calculated

$$B(\psi(2S) \to b_1^{\pm}\pi^{\mp}) = (3.0 \pm 0.5 \pm 0.7) \times 10^{-4},$$

where the first error is statistical and second systematic.

The decay $\psi(2S) \to \omega f_2$ is investigated on the $\pi^+\pi^-$ mass plot recoiling to ω of signal band (figure 7) and also of side band (figure 8). The $f_2(1270)$ signal is invisible on both plots. The f_2 signal has been fitted to a Breit-Wigner curve with width and mass fixed to PDG [2] added to quadratic background. Mass resolution is 12.3 MeV got by simulation. The fit leads to 2.3 ± 7.6 events. At the 90% confidence level the event number is less than 14.8. The efficiency is 0.076 calculated by simulation with uniform phase space distribution. Considering an isospin ratio 2:1 for f_2 decays into $\pi^+\pi^-$ or $\pi^0\pi^0$, one gets the branching fraction

$$B(\psi(2S) \to \omega f_2) < 1.1 \times 10^{-4} \qquad \text{(C.L.=90\%)}$$

IV. ANALYSIS OF $\psi(2S) \to \rho \mathbf{A}_2$

This decay channel is analyzed in $\rho^0\rho^{\pm}\pi^{\mp}$ combination which decays to $\pi^+\pi^-\pi^+\pi^-\pi^0$ final state. The $\rho^0\rho^{\pm}\pi^{\mp}$ candidate is selected by minimizing the quantity

$$\Delta = \sqrt{(m_{\pi^+\pi^-} - m_{\rho^0})^2 + (m_{\pi^0\pi^{\pm}} - m_{\rho^{\pm}})^2}$$

and a cut $\Delta < 110\ MeV/c^2$ is applied. Another range $130 < \Delta < 170\ MeV/c^2$ is selected for the side band of $\rho^{\pm}\pi^{\mp}\rho^0$ combination. The dalitz plots of $\rho^0\pi^{\pm}$ versus $\rho^{\mp}\pi^{\pm}$ are in figure 9 for the signal region and figure 10 for the side band. The $a_2(1320)$ signal is very marginal on the combining $\rho^0\pi^{\pm}$ and $\rho^{\pm}\pi^{\mp}$ mass plot from both $\rho^0\rho^{\pm}\pi^{\mp}$ candidate (figure 11) and $\rho^0\rho^{\pm}\pi^{\mp}$ side band (figure 12). A fit to a Breit-Wigner curve with a_2 mass and width fixed to PDG [2] over a quadratic background yields ρa_2 event number 6.2 ± 10.8. The event number is less than 23.9 at 90% confidence level. Simulation with uniform phase space distribution gives 0.046 detection efficiency. Assuming an isospin ratio of $a_2^+\rho^- : a_2^-\rho^+ : a_2^0\rho^0 = 1:1:1$ for $\psi(2S)$ decay, one calculates

$$B(\psi(2S) \to \rho a_2) < 3.0 \times 10^{-4},$$

V. ANALYSIS OF $\psi(2S) \to K^+K^-K^+K^-$

Events with four charged tracks (MFIT=2) in the polar angle region $-0.8 < \cos\theta < 0.8$ and with zero net charge have been selected. The dE/dx measurements are used to select kaon tracks with confidence level larger than 0.003 for each track and 0.01 for all tracks

combined. So are the TOF measurements of high quality ($T_{qual} = 1$). Magnetic field correction is made to momentum of charged track. Momentum correction is further made for energy loss and multiple Coulomb scattering in the material before track enters the drift volume in BES inner detector. Events are kinematically $4C$ fitted to improve mass resolution and exclude background. The probability of fit is required to be higher than 0.01. There remains 41 events after the above selections. No track seems to be electron ($E_{BSC}/P < 0.6$ when $P > 1GeV/c$) or muon (μ hit less than 2). The resulting dalitz plot (figure 13) shows ϕ signals. Figure 14 is the mass plot of K^+K^- (4 entries/event). The fit of guassian curve to K^+K^- mass plot gives ϕ number 16.3 ± 4.1. The mass resolution of ϕ is 6 MeV. The fitted mass of ϕ is $1019.4 \pm 1.9\ MeV/c^2$. Furthermore, the ϕ candidate is selected as $m_{K^+K^-} < 1040\ MeV/c^2$ to investigate the recoiling part. The mass plot of K^+K^- pair recoiling to ϕ (figure 15) shows ϕ signal although $f_2'(1525)$ is absent. Four entries of two events are in the ϕ mass range ($m_{K^+K^-} < 1040\ MeV/c^2$). The number of $\phi\phi$ events is less than 5.32 at 90% confidence level. The f_2' signal is fitted to a Breit-Wigner curve added to linear background with mass and width fixed to PDG. The mass resolution is 6 MeV. The fitted number of f_2' is 1.1 ± 2.3. At 90% confidence level the number is less than 4.9.

Simulations result in efficiencies 0.171 for $\psi' \to K^+K^-K^+K^-$, 0.175 for $\psi' \to \phi K^+K^-$, 0.231 for $\phi\phi$, 0.181 for $\phi f_2'(1525)$ respectively. The branching fractions are calculated

$$B(\psi' \to K^+K^-K^+K^-) = (6.5 \pm 1.0 \pm 0.9) \times 10^{-5}$$

$$B(\psi' \to \phi K^+K^-) = (5.1 \pm 1.3 \pm 0.9) \times 10^{-5}$$

$$B(\psi' \to \phi\phi) < 2.6 \times 10^{-5}$$

$$B(\psi' \to \phi f_2'(1525)) < 3.4 \times 10^{-5}$$

VI. SUMMARY AND DISCUSSION

The decays of $\psi(2S)$ to $2(\pi^+\pi^-)\pi^0$ and $K^+K^-K^+K^-$ have been studied from a high statistics constrained and fully reconstructed events. Three vector-tensor combinations, ωf_2, ρa_2 and $\phi f_2'(1525)$ are measured in $\psi(2S)$ decays. Moreover, the branching fraction of $\psi(2S)$ decays to $K^{*0}K_2^{*0}$ has also been measured by another BES analysis memo in $\psi(2S) \to \pi^+\pi^-K^+K^-$ channel [6]. Table I summarizes the results of branching ratio measured for $\psi(2S)$ decays into vector plus tensor combinations and also the PDG [2] values for the corresponding J/ψ decays. All four channels give values of the ratio of branching fractions of the $\psi(2S)$ to the J/ψ much lower than the prediction of perturbative QCD. As vector-tensor combinations, their suppressions provide a striking deviation from the naive expectation [1] and as yet there is no satisfactory theoretical explanation.

REFERENCES

[1] T. Applequist and D. Politzer, Phys. Rev. Lett. 34, 43(1975).
[2] R.M.Barnett et al. (Particle Data Group), Phys. Rev. D54, 1(1996).
[3] M.E.B.Franklin et al., Phys. Rev. Lett. 51, 963(1983).
[4] R.A.Lee, SLAC-PUB-3676, May 1985.
[5] G.Karl and W.Roberts, Phys. Lett. B144, 263(1984);
G.Karl and S.F.Tuan, Phys. Rev. D34, 1629(1986);
M.Chaichian et al., Nucl. Phys. B323, 75(1989);
S.S.Pinsky, Phys. Lett. B236, 479(1990);
W.S.Hou and A.Soni, Phys. Rev. Lett. 50, 569(1983);
S.J.Brodsky et al., Phys. Rev. Lett. 59, 621(1987);
X.Q.Li et al., Phys. Rev. D55, (1997) 1241;
S.J.Brodsky et al., hep-ph/9704379.
[6] Yuan Changzheng, $\psi(2S) \to \pi^+\pi^-K^+K^-$, BES analysis memo, 1996.

FIGURES

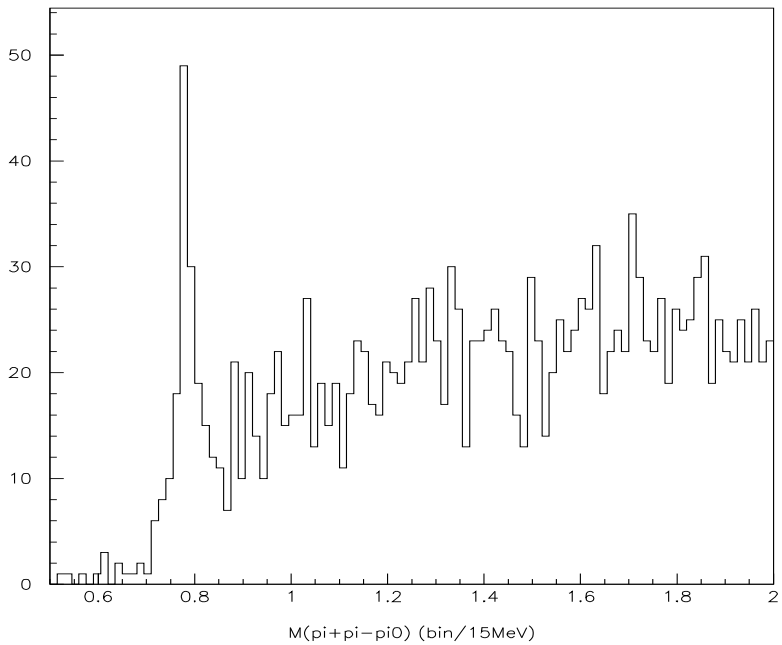

FIG. 1. Mass plot of $\pi^+\pi^-\pi^0$ in $\psi' \to \pi^+\pi^-\pi^+\pi^-\pi^0$

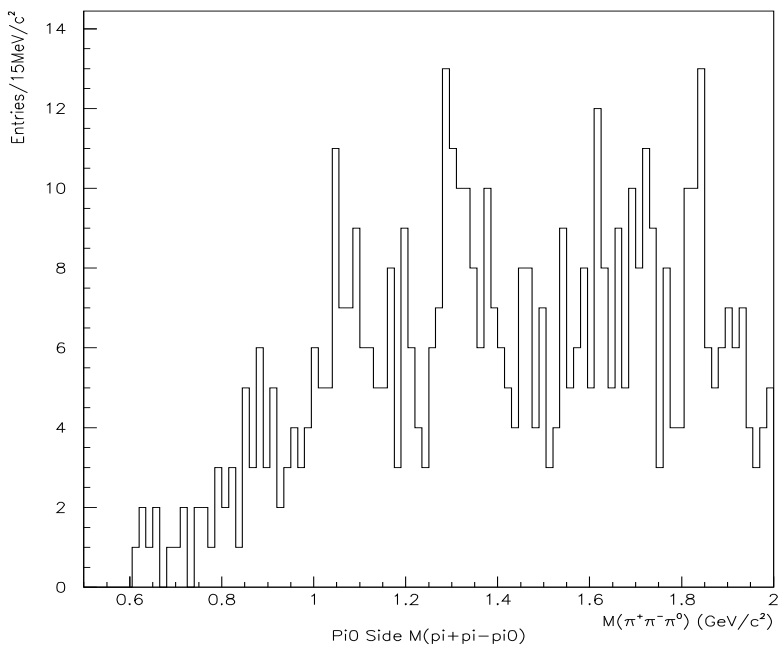

FIG. 2. Mass plot $\pi^+\pi^-\pi^0$ for the π^0 side band

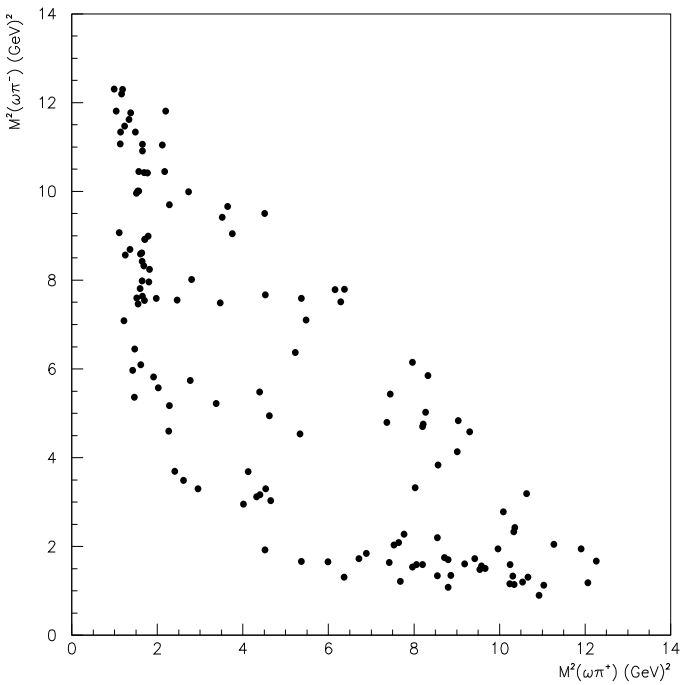

FIG. 3. Dalitz plot of $\omega\pi^+$ ves. $\omega\pi^-$.

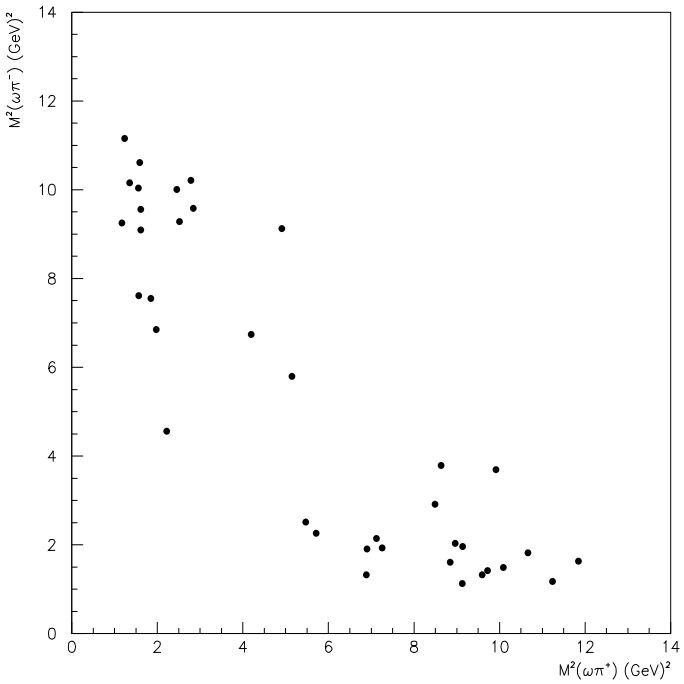

FIG. 4. Dalitz plot of $\omega\pi^+$ ves. $\omega\pi^-$ for π^0 side band.

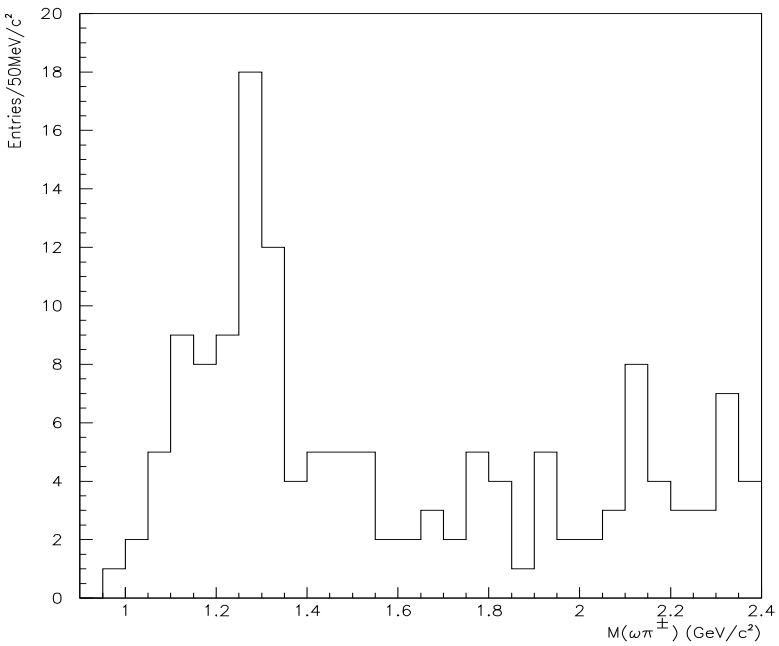

FIG. 5. $\omega\pi^{\pm}$ mass in $\psi' \to \omega\pi^{+}\pi^{-}$

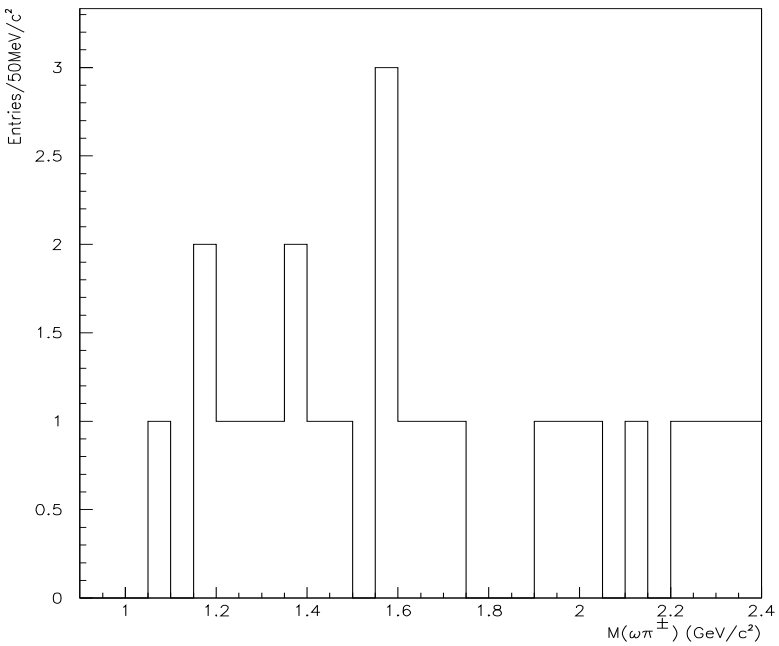

FIG. 6. $\omega\pi^{\pm}$ mass plot for the ω side band.

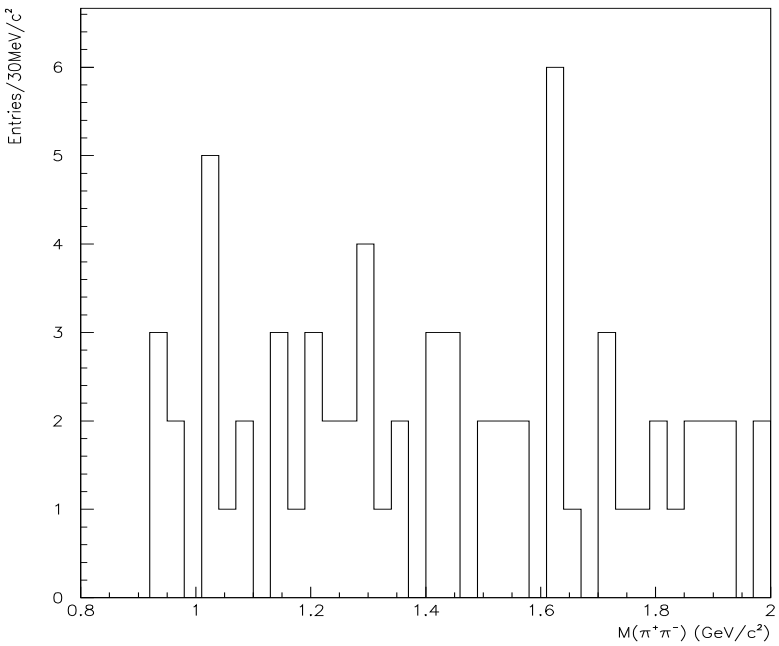

FIG. 7. Mass plot of $\pi^+\pi^-$ recoiling to ω in $\psi' \to \omega\pi^+\pi^-$

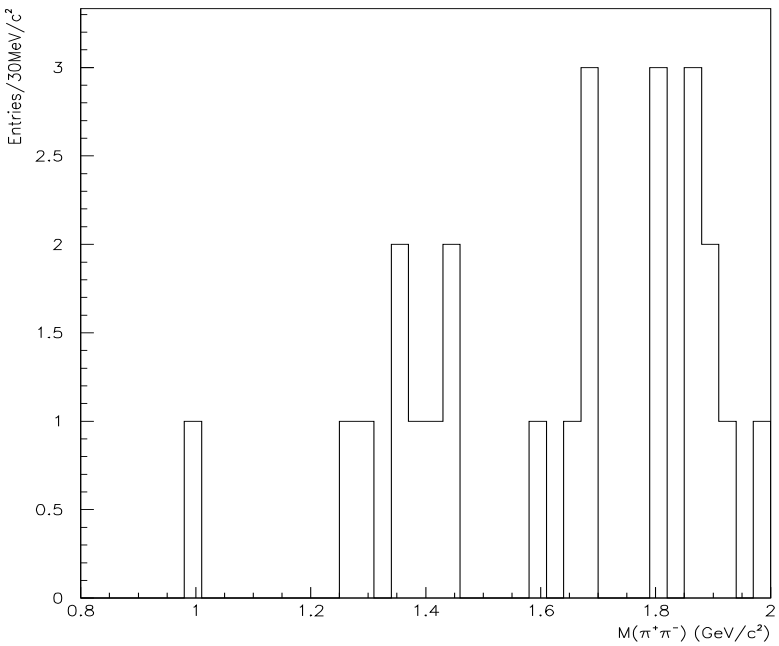

FIG. 8. Mass plot of $\pi^+\pi^-$ recoiling to ω side band

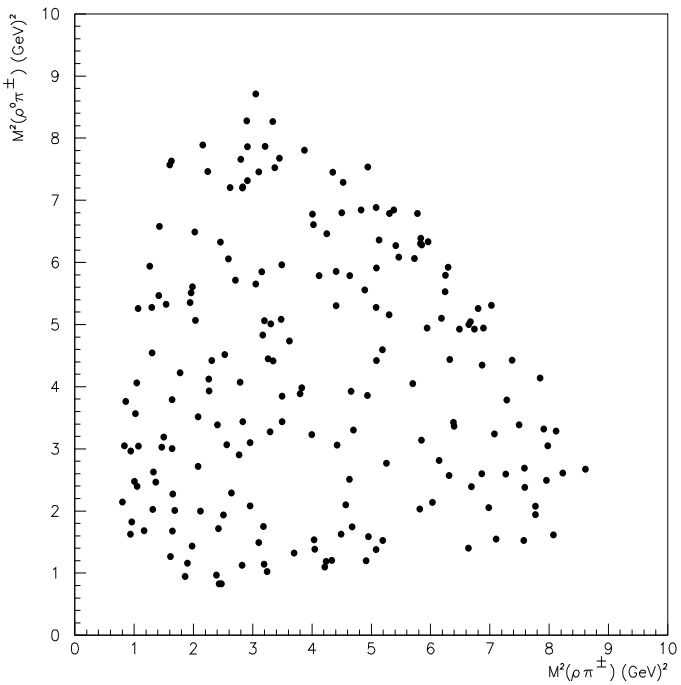

FIG. 9. Dalitz plot of $\rho^0\pi^\pm$ vers $\rho^\mp\pi^\pm$ in $\psi' \to \rho^0\rho^\mp\pi^\pm$

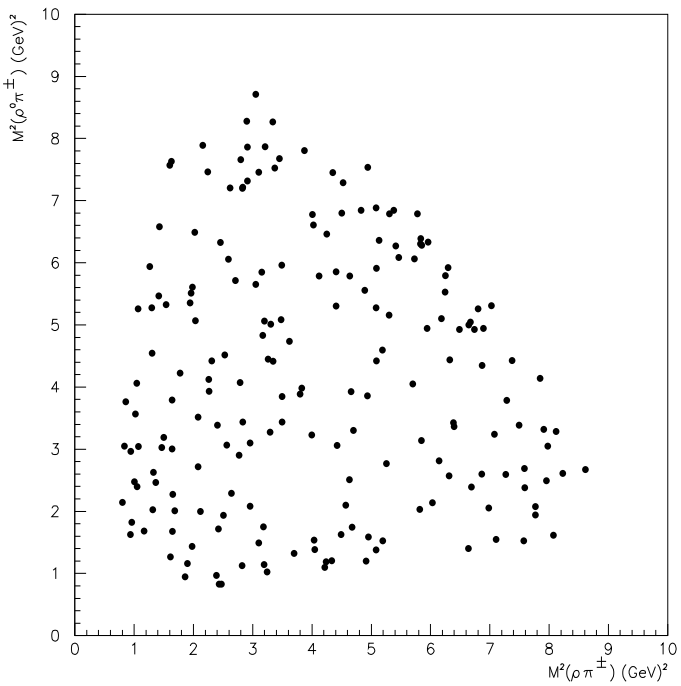

FIG. 10. Dalitz plot of $\rho^0\pi^\pm$ vers $\rho^\mp\pi^\pm$ for the side band of $\rho^0\rho^\mp\pi^\pm$ combination

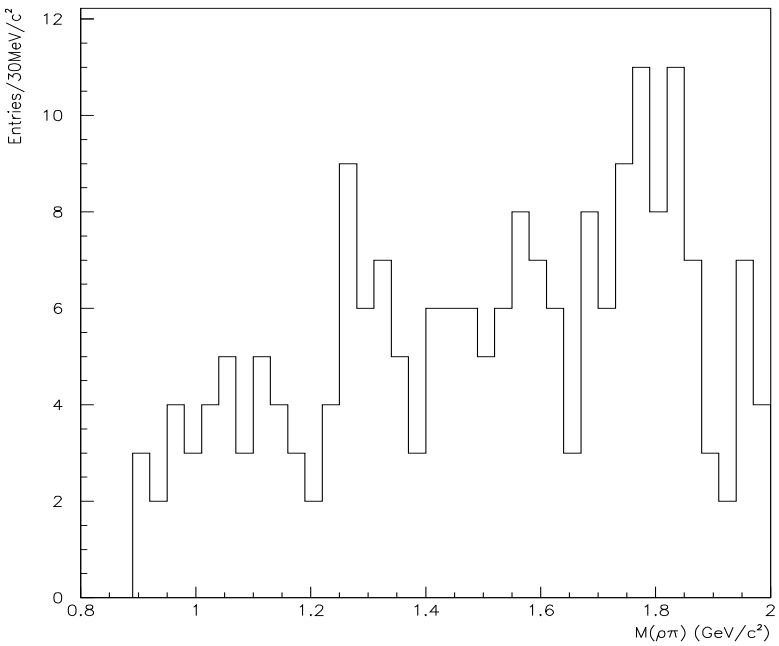

FIG. 11. Mass plot of $\rho\pi$ in $\psi' \to \rho^0\rho^{\mp}\pi^{\pm}$

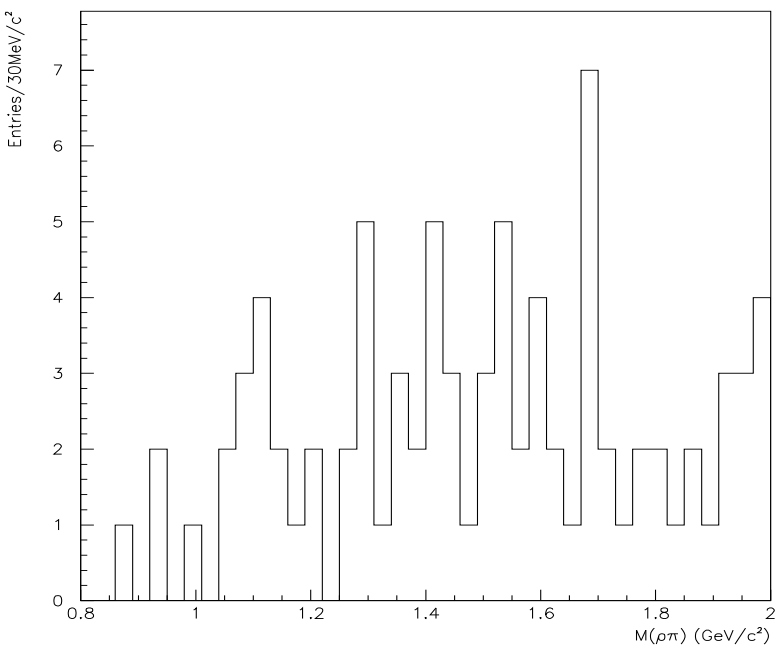

FIG. 12. Mass plot of $\rho\pi$ for the side band of $\rho^0\rho^{\mp}\pi^{\pm}$ combination

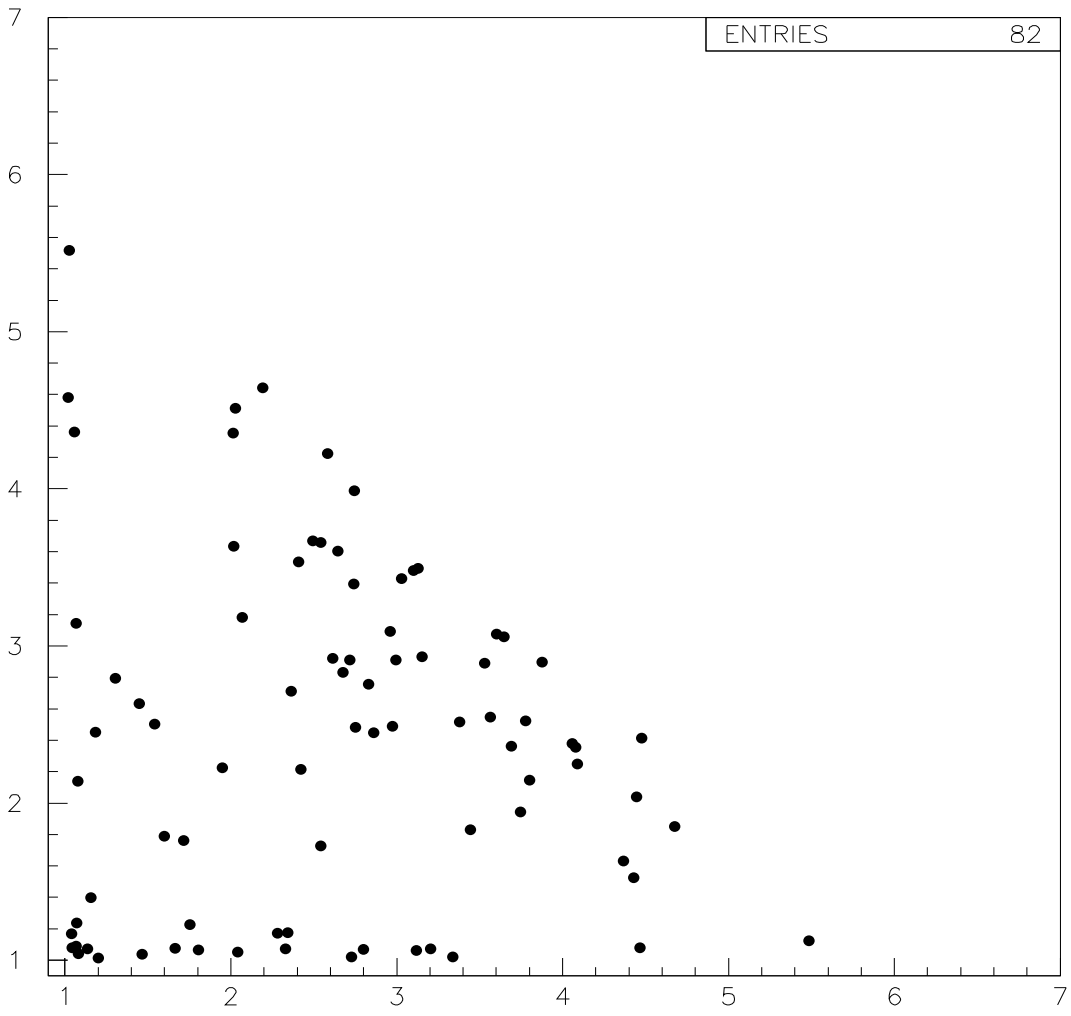

FIG. 13. Dalitz plot in $\psi' \to K^+K^-K^+K^-$

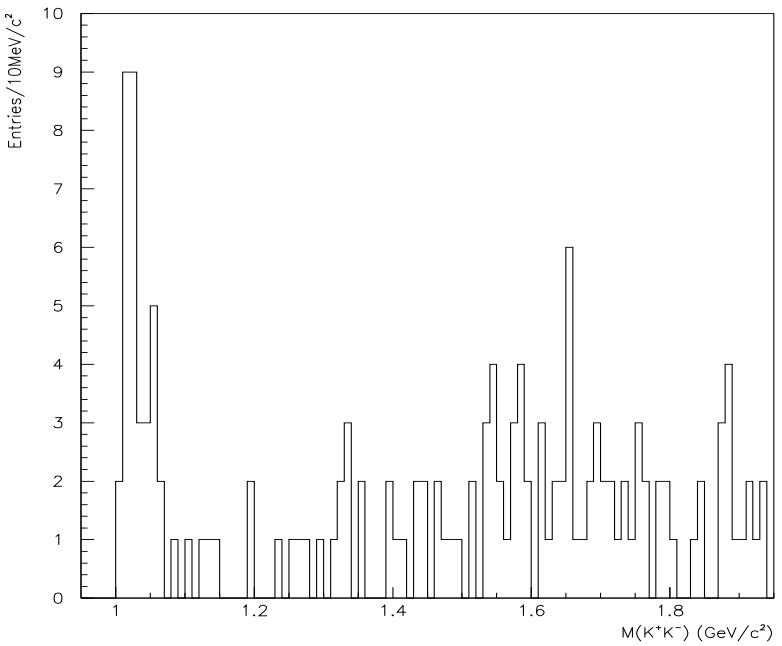

FIG. 14. K^+K^- mass in $\psi' \to K^+K^-K^+K^-$

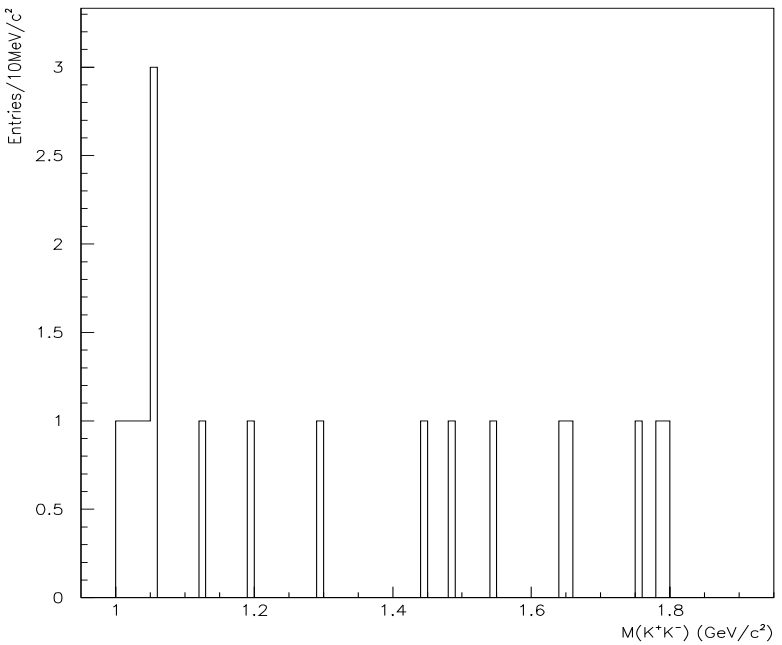

FIG. 15. Mass plot of K^+K^- recoiling to ϕ in $\psi' \to K^+K^-K^+K^-$

TABLES

	$B(\psi(2S))$	$B(J/\psi)$	$B(\psi(2S))/B(J/\psi)$
$\omega\pi^+\pi^-$	$(5.41 \pm 0.72 \pm 1.07) \times 10^{-4}$	$(7.2 \pm 1.0) \times 10^{-3}$	0.075 ± 0.021
ωf_2	$< 1.1 \times 10^{-4}$	$(4.3 \pm 0.6) \times 10^{-3}$	< 0.029
ρa_2	$< 3.0 \times 10^{-4}$	$(10.9 \pm 2.2) \times 10^{-3}$	< 0.028
$K^{*0}K_2^{*0} + c.c.$	$< 1.79 \times 10^{-4}$	$(6.7 \pm 2.6) \times 10^{-3}$	< 0.028
$\phi f_2'$	$< 4.9 \times 10^{-5}$	$(8 \pm 4) \times 10^{-4}$	< 0.045

TABLE I. Experimental ratios of $\psi(2S)$ compared to J/ψ (limits at 90% confidence level).